

Distribution of biomass dynamics in relation to tree size in forests across the world

Camille Piponiot^{1,2,3,✉}, Kristina J. Anderson-Teixeira^{2,4}, Stuart J. Davies^{1,5}, David Allen⁶, Norman A. Bourg², David F.R.P. Burslem⁷, Dairon Cárdenas⁸, Chia-Hao Chang-Yang⁹, George Chuyong¹⁰, Susan Cordell¹¹, Handanakere Shivaramaiah Dattaraja¹², Álvaro Duque¹³, Sisira Ediriweera¹⁴, Corneille Ewango¹⁵, Zacky Ezedin¹⁶, Jonah Filip¹⁷, Christian Giardina¹¹, Robert Howe¹⁸, Chang-Fu Hsieh¹⁹, Stephen Hubbell²⁰, Faith M. Inman-Narahari¹¹, Akira Itoh²¹, David Janík²², David Kenfack^{1,5}, Kamil Král²², James A. Lutz²³, Jean-Remy Makana¹⁵, Sean M. McMahon²⁴, William McShea², Xiangcheng Mi²⁵, Mohizah Bt. Mohamad²⁶, Vojtěch Novotný^{17,27}, Michael J. O'Brien²⁸, Rebecca Ostertag²⁹, Geoffrey Parker³⁰, Rolando Pérez¹, Haibao Ren²⁵, Glen Reynolds³¹, Mohamad Danial Md Sabri³², Lawren Sack²⁰, Ankur Shringi¹², Sheng-Hsin Su³³, Raman Sukumar³⁴, I-Fang Sun³⁵, Hebbalalu S. Suresh³⁴, Duncan W. Thomas³⁶, Jill Thompson³⁷, Maria Uriarte³⁸, John Vandermeer³⁹, Yunquan Wang⁴⁰, Ian M. Ware¹¹, George D. Weiblen¹⁶, Timothy J. S. Whitfeld⁴¹, Amy Wolf¹⁸, Tze Leong Yao³², Mingjian Yu⁴², Zuoqiang Yuan⁴³, Jess K. Zimmerman⁴⁴, Daniel Zuleta⁴, and Helene C. Muller-Landau¹

¹ Forest Global Earth Observatory, Smithsonian Tropical Research Institute, Apartado Postal 0843-03092, Panamá, Republic of Panamá

² Conservation Ecology Center, Smithsonian Conservation Biology Institute, Virginia 22630, USA

³ Cirad, Université de Montpellier, UR Forests and Societies, 34980 Montferrier-sur-Lez, France

⁴ Forest Global Earth Observatory, Smithsonian Tropical Research Institute, Washington, DC 20560, USA

⁵ Department of Botany, National Museum of Natural History, Washington, DC 20560, USA

⁶ Department of Biology, Middlebury College, Middlebury, Vermont 05753, USA

⁷ School of Biological Sciences, University of Aberdeen, Aberdeen AB24 3UU, United Kingdom

⁸ Instituto Amazónico de Investigaciones Científicas Sinchi, Bogotá, DC, Colombia

This is the author manuscript accepted for publication and has undergone full peer review but has not been through the copyediting, typesetting, pagination and proofreading process, which may lead to differences between this version and the Version of Record. Please cite this article as doi: [10.1111/NPH.17995](https://doi.org/10.1111/NPH.17995)

This article is protected by copyright. All rights reserved

- ⁹ Department of Biological Sciences, National Sun Yat-sen University, Kaohsiung City 80424
- ¹⁰ Department of Botany and Plant Physiology, University of Buea, Buea, Cameroon
- ¹¹ Institute of Pacific Islands Forestry, USDA Forest Service, Hilo, Hawai`i 96720, USA
- ¹² Centre for Ecological Sciences, Indian Institute of Science, Bangalore, Karnataka, India
- ¹³ Departamento de Ciencias Forestales, Universidad Nacional de Colombia Sede Medellín, Medellín, Colombia
- ¹⁴ Department of Science and Technology, Faculty of Applied Sciences, Uva Wellassa University, Badulla 90000, Sri Lanka
- ¹⁵ Faculty of Sciences, University of Kisangani, BP 2012 Kisangani, DR Congo
- ¹⁶ Department of Plant & Microbial Biology, University of Minnesota, St. Paul, Minnesota 55108, USA
- ¹⁷ Binatang Research Centre, Madang, Papua New Guinea
- ¹⁸ Department of Natural and Applied Sciences, University of Wisconsin-Green Bay, Green Bay, Wisconsin 54311-7001, USA
- ¹⁹ Institute of Ecology and Evolutionary Biology, National Taiwan University, Taipei 10617
- ²⁰ Department of Ecology and Evolutionary Biology, University of California, Los Angeles, Los Angeles, California 90095, USA
- ²¹ Graduate School of Science, Osaka City University, Osaka 5588585, Japan
- ²² Department of Forest Ecology, Silva Tarouca Research Institute, Brno 602 00, Czech Republic
- ²³ Wildland Resources Department, Utah State University, Logan, Utah 84322, USA
- ²⁴ Forest Global Earth Observatory, Smithsonian Environmental Research Center, Edgewater, Maryland 21037, USA
- ²⁵ State Key Laboratory of Vegetation and Environmental Change, Institute of Botany, Chinese Academy of Sciences, Xiangshan, Beijing 100093
- ²⁶ Research Development and Innovation Division, Forest Department Sarawak, Bangunan Baitul Makmur 2, Medanraya, Petrajaya, 93050 Kuching, Malaysia
- ²⁷ Biology Centre, Academy of Sciences of the Czech Republic and Faculty of Science, University of South Bohemia, Ceske Budejovice 37005, Czech Republic
- ²⁸ Área de Biodiversidad y Conservación, Universidad Rey Juan Carlos, Móstoles 28933, Spain
- ²⁹ Department of Biology, University of Hawaii, Hilo, Hawai`i 96720, USA
- ³⁰ Forest Ecology Group, Smithsonian Environmental Research Center, Edgewater, Maryland

21037, USA

³¹ The Royal Society SEARRP (UK/Malaysia), Danum Valley, Malaysia

³² Forestry and Environment Division, Forest Research Institute Malaysia, Kepong, Selangor, Malaysia

³³ Taiwan Forestry Research Institute, Taipei 100051

³⁴ Centre for Ecological Sciences and Divecha Centre for Climate Change, Indian Institute of Science, Bangalore, Karnataka, India

³⁵ Department of Natural Resources and Environmental Studies, National Dong Hwa University, Hualien 974301

³⁶ School of Biological Sciences, Washington State University, Vancouver, Washington 99164, USA

³⁷ UK Centre for Ecology and Hydrology, Bush Estate, Penicuik, Midlothian EH26 0SB, United Kingdom

³⁸ Department of Ecology, Evolution, and Environmental Biology, Columbia University, New York, New York 10027, USA

³⁹ Department of Ecology and Evolutionary Biology and Herbarium, University of Michigan, Ann Arbor, Michigan 48109, USA

⁴⁰ College of Chemistry and Life Sciences, Zhejiang Normal University, Jinhua 321004

⁴¹ Bell Museum, University of Minnesota, St. Paul, Minnesota 55108, USA

⁴² College of Life Sciences, Zhejiang University, Hangzhou

⁴³ CAS Laboratory of Forest Ecology and Management, Institute of Applied Ecology, Chinese Academy of Sciences, Shenyang, 110016

⁴⁴ Department of Environmental Sciences, University of Puerto Rico, San Juan, Puerto Rico

Author for correspondence: Camille Piponiot <camille.piponiot-laroche@cirad.fr>

Received: 9 April 2021

Accepted: 5 October 2021

Individual ORCID IDs

Author	ORCID
Camille Piponiot	0000-0002-3473-1982
Kristina J. Anderson-Teixeira	0000-0001-8461-9713
Stuart J. Davies	0000-0002-8596-7522
David Allen	0000-0002-0712-9603
Norman A. Bourg	0000-0002-7443-1992
David F.R.P. Burslem	0000-0001-6033-0990
Chia-Hao Chang-Yang	0000-0003-3635-4946
Susan Cordell	0000-0003-4840-8921
Sisira Ediriweera	0000-0002-2270-6085
Christian Giardina	0000-0002-3431-5073
Robert Howe	0000-0001-8393-4981
Chang-Fu Hsieh	0000-0003-4165-8100
Akira Itoh	0000-0002-2493-1681
David Jánik	0000-0002-8271-7456
David Kenfack	0000-0001-8208-3388
Kamil Král	0000-0002-3848-2119
James A. Lutz	0000-0002-2560-0710
Jean-Remy Makana	0000-0002-6006-2938
Sean M. McMahon	0000-0001-8302-6908

William McShea	0000-0002-8102-0200
Xiangcheng Mi	0000-0002-2971-5881
Mohizah Bt. Mohamad	0000-0003-1645-2469
Vojtěch Novotný	0000-0001-7918-8023
Michael J. O'Brien	0000-0003-0943-8423
Rebecca Ostertag	0000-0002-5747-3285
Lawren Sack	0000-0002-7009-7202
Sheng-Hsin Su	0000-0003-1337-3335
I-Fang Sun	0000-0001-9749-8324
Duncan W. Thomas	0000-0003-1818-0057
Jill Thompson	0000-0002-4370-2593
Maria Uriarte	0000-0002-0484-0758
Ian M. Ware	0000-0002-2101-5653
George D. Weiblen	0000-0002-8720-4887
Timothy J. S. Whitfeld	0000-0003-1850-6432
Amy Wolf	0000-0001-8983-8181
Zuoqiang Yuan	0000-0001-9197-7076
Daniel Zuleta	0000-0001-9832-6188
Helene C. Muller-Landau	0000-0002-3526-9021

Summary

- Tree size shapes forest carbon dynamics and determines how trees interact with their environment, including a changing climate. Here we conduct the first global analysis of among-site differences in how aboveground biomass stocks and fluxes are distributed with tree size.
- We analyzed repeat tree censuses from 25 large-scale (4-52 ha) forest plots spanning a broad climatic range over five continents to characterize how aboveground biomass, woody productivity and woody mortality vary with tree diameter. We examined how the median, dispersion and skewness of these size-related distributions vary with mean annual temperature and precipitation.
- In warmer forests, aboveground biomass, woody productivity and woody mortality were more broadly distributed with respect to tree size. In warmer and wetter forests, aboveground biomass and woody productivity were more right-skewed, with a long tail towards large trees. Small trees (1-10 cm diameter) contributed more to productivity and mortality than to biomass, highlighting the importance of including these trees in analyses of forest dynamics.
- Our findings provide an improved characterization of climate-driven forest differences in the size structure of aboveground biomass and dynamics of that biomass, as well as refined benchmarks for capturing climate influences in vegetation demographic models.

Key words: biomass; climate gradients; forests; tree size distribution; woody productivity; woody mortality.

Introduction

Forests are highly size-structured: tree size influences access to resources and impact of disturbances, and thereby growth and mortality rates (Muller-Landau *et al.*, 2006a; Anderson-Teixeira *et al.*, 2015b; Stark *et al.*, 2015). Larger diameter trees generally have access to higher light environments, which in turn enables greater tree growth rates (Stark *et al.*, 2012). However, larger trees also tend to be more vulnerable to drought (Bennett *et al.*, 2015; McGregor *et al.*, 2021) and to wood-boring insects (Pfeifer *et al.*, 2011), and their crowns are more exposed to

lightning strikes (Gora *et al.*, 2020; Yanoviak *et al.*, 2020) and to winds that can cause windthrow (Gardiner *et al.*, 2005; Gora & Esquivel-Muelbert, 2021). In contrast, smaller trees are more likely to die from competition-induced carbon starvation (McDowell *et al.*, 2018), from neighboring trees and falling branches (Meer & Bongers, 1996), and may be more vulnerable to fire (Brando *et al.*, 2012; Hood *et al.*, 2018).

Among-site differences in climate, disturbance intensity, and other drivers lead to variation in the size-dependence of tree growth and mortality rates, and thus in tree size distributions and the distribution of aboveground biomass (AGB), woody productivity and woody mortality fluxes with tree size (Muller-Landau *et al.*, 2006b; Meakem *et al.*, 2018; Gora *et al.*, 2020). Critically, as climate change and anthropogenic disturbances alter resource availability (e.g. water and light) and disturbance regimes (Lewis *et al.*, 2015; Seidl *et al.*, 2017), the size structure of forests will modulate forest carbon cycle responses. For example, climate change that increases stresses and thus mortality rates of large trees will have greater impact on forests with larger concentrations of biomass and productivity in large trees. Understanding the distribution of carbon stocks and fluxes with tree size is thus a foundation for accurately quantifying current and future forest carbon stocks and cycling, and for projecting climate change feedbacks to these measures (Zuidema *et al.*, 2013). Consistent, comparative data on size-related carbon stocks and fluxes for multiple forests are also particularly valuable today as benchmarks for the size-dependent demographics of vegetation models, which are increasingly used to represent vegetation dynamics in Earth system models (Fisher *et al.*, 2018).

Tree size distributions vary strongly with climate among sites, as do size-specific growth and mortality rates, and thus the distributions of carbon stocks and fluxes with tree size vary as well. Large trees are typically more abundant and contribute a greater proportion of AGB in warmer, lower latitude forests (Lutz *et al.*, 2018). The proportion of large trees also increases with precipitation (Segura *et al.*, 2002), likely due to the greater sensitivity of large trees to water stress (Bennett *et al.*, 2015). Abundances of small trees also vary among sites; they are higher in wet or moist tropical forests than in temperate forests (King *et al.*, 2006). This may be because these aseasonal environments enable longer (multi-year) leaf lifespans of broadleaved understory trees (Coley, 1988), which effectively reduce the cost of deploying leaves, and thereby enable survival even in low-light environments. Moreover, shade tolerance, i.e., the ability to survive

and grow in low-light environments, increases in strength with the length of the growing season and is inversely related to tolerance to other environmental stresses such as drought (Valladares & Niinemets, 2008). Given these patterns, we expect distributions of forest AGB with tree size to be more dispersed and right-skewed, that is a greater proportion of small trees and a longer tail to large trees, in warmer, wetter forests. We expect similar size distributions in annual AGB fluxes, i.e. aboveground woody productivity (AWP, the flux in AGB associated with tree growth and recruitment) and mortality (AWM, the flux from AGB to necromass due to mortality), when conditions are relatively stable.

Yet, we expect size distributions of AWP and AWM to be shifted towards smaller size classes relative to AGB. Studies across many different forest types and tree species have observed decreasing productivity per unit biomass with tree size (e.g., Mencuccini *et al.*, 2005; Kohyama *et al.*, 2020). This occurs even though absolute productivity generally continues to increase with tree size (e.g., Stephenson *et al.*, 2014), because productivity increases more slowly than biomass. Our focus here is on aboveground woody productivity per aboveground biomass (AWP/AGB), henceforth relative aboveground woody productivity (RAWP). Multiple mechanisms can contribute to reductions in RAWP with tree size, including lower ratios of leaf area to stem mass (Poorter *et al.*, 2015a), higher maintenance costs (Magnani *et al.*, 2000), increasing hydraulic limitation (Drake *et al.*, 2010), and allocation shifts towards reproduction and other non-woody tissues (Ryan *et al.*, 2004; Thomas, 2011). The contributions and strengths of these mechanisms, and thus the strength of the decline in RAWP with tree size, is likely to vary among sites and species. However, few studies have specifically quantified stand-level patterns of RAWP with tree size, much less compared them among sites (but see Meakem *et al.*, 2018). In old-growth forests at steady state, in which size distributions are not changing directionally, productivity and mortality at a given size class are on average equal, and thus we expect patterns for relative aboveground woody mortality (RAWM = AWM/AGB) with tree size to follow those of RAWP.

To our knowledge, no study has investigated how stand-level stocks and fluxes of aboveground biomass (the largest and most easily estimated tree carbon pool) are distributed by tree size across a large variety of forest types and biomes. Previous studies have analyzed among-site variation in total stand-level AGB stocks and fluxes (Banbury Morgan *et al.*, 2021; Muller-Landau *et al.*,

2021; Anderson-Teixeira *et al.*, 2021), and in tree size distributions (i.e., the densities of trees of different sizes; e.g., Muller-Landau *et al.*, 2006b). Studies have also quantified total AGB stocks and fluxes in one particular size class – large trees – and have shown that they contain a large proportion of the AGB (Slik *et al.*, 2013; Lutz *et al.*, 2018; Mildrexler *et al.*, 2020), and are good predictors of forest structure (Bastin *et al.*, 2018). However, very few studies have examined the relative contribution of all tree sizes to both AGB stocks and fluxes, even though smaller trees can also have a role in shaping AGB dynamics (Newbery *et al.*, 2013; Hubau *et al.*, 2019; Mensah *et al.*, 2020). Rare exceptions include a study quantifying size-related distributions of AGB, AWP, and AWM in three forest plots along a precipitation gradient in Panama (Meakem *et al.*, 2018).

In this study, we quantified how AGB, AWP, and AWM are distributed with respect to tree diameter at breast height (DBH) in large-scale (4-52 ha) forest plots across the world belonging to the ForestGEO network of large forest plots (<https://forestgeo.si.edu>, Davies *et al.*, 2021; Anderson-Teixeira *et al.*, 2015a), and tested associated hypotheses. We quantified the median, dispersion and skewness of distributions of each variable with DBH, and investigated how they vary among sites with climate. We examined how relative AWP (RAWP=AWP/AGB) and relative AWM (RAWM=AWM/AGB) vary with DBH and among sites. We also specifically quantified the relative importance of the smallest (≥ 1 cm but < 10 cm DBH) and largest (≥ 60 cm DBH) trees for aboveground biomass stocks and fluxes. We expected size-related distributions of AGB, AWP and AWM to be more dispersed and right-skewed, that is a greater proportion of small trees and a longer tail to large trees, in warmer, wetter forests (Hypothesis 1). Thus, we specifically expected the skewness and dispersion of the size-related distributions to increase with MAT and MAP (Hypothesis 1a), and to be higher in tropical than temperate forests (Hypothesis 1b). We also expected RAWP and RAWM to decrease with tree diameter in all sites, such that although large trees dominate biomass stocks and fluxes, small trees are proportionally more important to AWP and AWM than they are to AGB (Hypothesis 2a). Consistent with this, we expected the probability distributions of AWP and AWM to be shifted towards smaller size classes than those of AGB (lower medians; Hypothesis 2b), the contributions of the smallest trees (≥ 1 cm but < 10 cm DBH) to AWP to be larger than their contributions to AGB (Hypothesis 2c), and the contributions of the largest trees (≥ 60 cm DBH) to AWP to be smaller than their contributions to AGB (Hypothesis 2d).

Materials and Methods

Study sites and data

Repeated tree censuses were conducted in 25 forest plots (Table 1; Supporting information, Fig. S1 and Table S1) distributed across 5 continents following a standardized protocol (Condit, 1998; Davies *et al.*, 2021). Plots are located in old-growth or mature secondary forests, and several have been subjected to some level of natural and/or historical human disturbances (Anderson-Teixeira *et al.*, 2015a, Table S2), although we lack consistent, quantitative data on the intensity, size-selectivity, and timing of those disturbances at each site. All stems ≥ 1 cm diameter at breast height (DBH; diameter at 1.3 m height or above any stem irregularities) were mapped, tagged, identified to genus or species, and measured in DBH. For stems measured at a height > 1.3 m in tropical sites, we applied a taper correction to estimate the equivalent DBH at 1.3 height following Cushman *et al.* (2021). We excluded lianas, tree ferns and strangler figs from the analysis. We analyzed data for the most recent census interval at each site, or the next-to-last interval if the most recent census interval had been affected by a major disturbance (e.g., El Niño drought in Cocoli; Meakem *et al.*, 2018). Climate variables were provided by each site (Table 1, Anderson-Teixeira *et al.*, 2015a; Davies *et al.*, 2021).

We estimated total aboveground biomass (AGB) for each tree at each census from the measured DBH using the pantropical allometric equation from Chave *et al.* (2014) and Réjou-Méchain *et al.* (2017) for tropical sites, and the generalized allometric equations from Chojnacky *et al.* (2014) for other sites. For all tropical sites (except Fushan) we used equation 7 from Chave *et al.* (2014), that does not include height as an input variable. For the Fushan site, where frequent typhoons result in lower tree height than the global prediction, we used a local height allometry (McEwan *et al.*, 2011) in combination with equation 4 from Chave *et al.* (2014). For temperate sites, we used the equations in Table 5 of Chojnacky *et al.* (2014), which rely on information on wood density and taxonomic identity. Each tree was assigned a wood density, based on its taxonomic identity, from the Global Wood Density Database (Zanne *et al.*, 2009) using the R package BIOMASS (Réjou-Méchain *et al.*, 2017). Unidentified trees and trees that lacked a species- or genus-level wood density value in the database were assigned a stand-level mean wood density over all individuals.

Size-related stand dynamics

We calculated total aboveground biomass stocks and fluxes by 20 x 20 m quadrats and 1 cm diameter classes. Specifically, we examined the following variables: (i) aboveground biomass (AGB, $\text{Mg ha}^{-1} \text{cm}^{-1}$), (ii) aboveground woody productivity, i.e. annual Mg increment from stem growth of surviving trees and recruitment (AWP, $\text{Mg ha}^{-1} \text{yr}^{-1} \text{cm}^{-1}$), (iii) aboveground woody mortality (AWM, $\text{Mg ha}^{-1} \text{yr}^{-1} \text{cm}^{-1}$). We corrected for bias induced by different lengths of census interval using a method described in Kohyama *et al.* (2019), and gap-filled unrealistically large changes in measured DBH with the expected DBH change for the corresponding size class and site (Supporting information, Methods S1, S2; Figs. S2, S3). For graphical visualization (but not for analysis), we aggregated data into wider size classes, with size class boundaries defined separately for each site, based on the total number of stems and their distribution with size (Supporting information, Methods S3, Table S3, Fig. S4). Values were standardized per cm of diameter class width (i.e., dividing size class totals by the width of the diameter size class in cm).

To summarize size distribution patterns for each variable and site, we calculated the median, dispersion and skewness of each distribution. The median is the DBH at which 50% of the total stock or flux is below, and 50% above. We calculated the dispersion as the quartile coefficient of dispersion (dimensionless), i.e. the difference between the third and first quartiles, divided by the sum of the first and third quartiles. We calculated the skewness as Pearson's first skewness coefficient (dimensionless), i.e. the difference between the mean and median of the distribution, divided by its standard deviation. These summary statistics (median, dispersion and skewness) were calculated based on 1-cm wide diameter classes. We analyzed the relationship of these summary statistics (median, dispersion and skewness) with climate by performing multiple linear regressions with the mean annual temperature (MAT) and precipitation (MAP) recorded at each site (Table 1; Supporting information, Table S4). MAT and MAP were chosen as climate variables because they are commonly used, and each were available on a site-by-site basis. However, these two variables are moderately correlated in our data (Pearson correlation coefficient = 0.53). To evaluate the robustness of our results to the chosen climate variables, we also performed multiple linear regressions with the MAT and an alternative moisture variable,

Selyaninov Hydrothermal Coefficient (SHC), that takes into account the effect of temperature on evapotranspiration (Supporting information, Table S5). SHC values were extracted at a 1-km resolution from the CHELSA database (Karger *et al.*, 2017). We tested for differences between tropical and temperate forests in the summary statistics (median, dispersion and skewness) for AGB, AWP and AWM by performing Wilcoxon signed-rank tests (Table S6). We tested whether the medians of AGB were larger than the medians of AWP and AWM by performing Wilcoxon signed-rank tests. To quantify the importance of small ($1 \text{ cm} \leq \text{DBH} < 10 \text{ cm}$) and large ($\text{DBH} \geq 60 \text{ cm}$) trees, we calculated their contributions as proportions of total AGB, AWP, and AWM. We also explored two other definitions of large trees: (i) the top 5% of trees with $\text{DBH} \geq 10 \text{ cm}$ and (ii) the largest trees that account for 50% of the stand AGB (following Lutz *et al.* (2018); Supporting information, Table S7, Figs. S5, S6).

Because of their relevance to understanding the distribution of AGB, AWP, and AWM with size, we also calculated the following variables by aggregated size classes (as defined in Supporting Information, Methods S3): relative AWP (RAWP, $\% \text{ yr}^{-1}$) defined as the ratio of AWP to AGB, relative AWM (RAWM, $\% \text{ yr}^{-1}$) defined as the ratio of AWM to AGB, mean individual stem AGB (Mg), and mean stem diameter growth (cm yr^{-1} ; Supporting information, Notes S1 and Figs. S7, S8, S9).

We calculated 95% confidence intervals on all variables by bootstrapping over 20 x 20 m quadrats with 1000 replicates. Static variables such as AGB were calculated based on the initial census of the focal census interval.

Results

Climate and size-related distributions of biomass stocks and fluxes

The distributions of AGB stocks and fluxes across size classes peaked at intermediate size classes in all sites, were very uneven, and varied strongly among sites (Fig. 1). In comparison with the temperate sites, tropical forests had a greater share of their total AGB and AWP in the small stems ($1 \leq \text{DBH} < 10 \text{ cm}$), and had more very large stems that store large amounts of AGB but made relatively smaller contributions to AWP (Fig. 4c). Most temperate sites (with the exception of Wind River) accumulated AGB between censuses and their net change in AGB (calculated as $\text{AWP} - \text{AWM}$) was positive (Supporting information, Fig. S10).

As expected (Hypothesis 1a), dispersion and skewness of AGB and AWP distributions generally increased with mean annual temperature and precipitation (MAT and MAP; Fig. 2). Multiple regression analyses found significant positive effects of both MAT and MAP on the dispersion of AGB distributions (Fig. 2a,b) and on the skewness of AWP distributions (Fig. 2g,h), i.e. AGB was more broadly distributed between size classes and AWP distributions were more right-skewed at higher MAT and higher MAP. There was also a significant positive effect of MAT on the dispersion of AWP and AWM distributions (Fig. 2c; Supporting information, Table S4), and a significant positive effect of MAP on the skewness of AGB distributions (Fig. 2f). MAT and MAP had no significant effect on the skewness of AWM or the medians of AGB, AWP or AWM (Fig. 2; Supporting information, Table S4). Consistent with these results and with Hypothesis 1b, the dispersion and skewness of AGB, AWP and AWM were significantly higher in tropical vs temperate forests, but the medians were not significantly different (Supporting information, Table S6).

Relative aboveground biomass fluxes as a function of tree size

Across all sites, RAWP decreased with increasing tree size: small trees had on average higher AWP relative to their AGB than large trees (Fig. 3a,b), consistent with Hypothesis 2a. RAWM also decreased with tree size in most sites (Fig. 3c,d), paralleling the patterns for the stem mortality rate (Supporting information, Fig. S9a and Notes S1). However, in some tropical sites (Pasoh, Korup, Wanang, Sinharaja) the curve was U-shaped, with RAWM being the highest for small and large trees, and the lowest for intermediate tree sizes. In the Zofin temperate site (Czech Republic), RAWM was particularly low for small trees and increased with tree size (under $0.3\% \text{ yr}^{-1}$ for all diameter classes $< 25 \text{ cm DBH}$; Fig. 3d).

The median of the AGB distribution was greater than (23/25) or equal to (2/25) the median of the AWP distribution in all 25 sites, and across sites the difference between the medians was significantly greater than zero (W -statistic = 276; p -value = 2.8510^{-5}), consistent with Hypothesis 2b. The AGB median was larger than the AWM median in 14 of 25 sites, but overall the difference between the medians of AGB and AWM was not significantly greater than zero (W -statistic = 195.5; p -value = 0.381).

The roles of large and small trees in biomass stocks and fluxes

As expected, large trees (≥ 60 cm DBH) contributed a large fraction to all biomass stocks and fluxes, while small trees (< 10 cm DBH) typically contributed $< 15\%$ (Fig. 4). Across all sites, small trees contributed more to AWP than to AGB (Fig. 4a), with contributions to AWP being typically twice AGB contributions, consistent with Hypothesis 2c. Conversely, large trees contributed less to AWP than to AGB (Fig. 4c), consistent with Hypothesis 2d. Small trees also contributed relatively more to AWM than to AGB in most sites (Fig. 4b), whereas large trees contributed similarly to AWM and AGB (Fig. 4d). Results were qualitatively similar for the two other definitions of large trees: (i) the largest trees that comprise 50% of the total AGB, and (ii) the top 5% of stems ≥ 10 cm (Supporting information, Table S7 and Figs. S5, S6).

To provide a resource for model benchmarking and simple comparisons among sites, we calculate size class values of all variables (AGB, AWP, AWM, and mean stem diameter growth) and their 95% confidence intervals for standardized diameter classes of [1,5), [5,10), [10,20), [20,30), [30,40), [40,50), [50,100), [100,200), and [200, $+\infty$) cm DBH (Supporting information, Dataset S2) in addition to the site-specific diameter classes presented in the main text (Supporting information, Dataset S1).

Discussion

Understanding among-site variation

Our results show that the size-related distributions of aboveground biomass stocks (AGB) and fluxes associated with growth (AWP) and mortality (AWM) vary substantially among sites. Climate explained considerable among-site variation in the size-related distribution of AWP. In warmer, wetter climates, the size-related distributions of AGB and AWP had higher dispersion and were more right-skewed (supporting Hypothesis 1), reflecting the presence of a dense understory and some very large trees. These results were consistent with results from previous studies (Segura *et al.*, 2002; King *et al.*, 2006; Lutz *et al.*, 2018) and with expected patterns of increased growth and survival of small understory trees (Valladares & Niinemets, 2008) as well as very large trees (Bennett *et al.*, 2015; Koch *et al.*, 2004) in forests with higher water availability and longer growing seasons. In addition, many temperate forests have high population densities of deer and other meso-herbivores (due to missing or reduced abundances of

their predators, Côté *et al.*, 2004; Estes *et al.*, 2011), and browsing by these herbivores may also contribute to low understory tree densities in these sites (McGarvey *et al.*, 2013). Another factor that may contribute to the observed patterns is that many of our temperate sites (which are colder and in many cases have lower precipitation than tropical sites; Table 1) are late-succession secondary forests that might lack very large trees, and thus have less dispersed distributions of AGB with tree size (Table S2).

Soil substrate, disturbance regime, species composition, and other factors also influence AGB dynamics and their distribution as a function of tree size, within and among sites. A more stable soil substrate (e.g., deeper soils and flatter topography) could decrease the probability of windthrows, thus allowing trees to grow larger and dominate biomass fluxes: this effect has been proposed as an explanation of basin-wide variations in Amazonian forests' structure (Quesada *et al.*, 2012), and may explain why small trees dominate biomass dynamics in the Wanang plot that experiences frequent and severe disturbances (Fig. 1; Supporting information, Fig. S10 and Table S2; Vincent *et al.*, 2018). Forest composition and diversity are also expected to have an important role in shaping size-related distributions of biomass stocks and fluxes (Poorter *et al.*, 2015b). For example, Southeast Asian forests dominated by Dipterocarpaceae had some of the largest trees and highest AWP among our sites (Danum Valley, Lambir, Pasoh, Sinharaja; Table 1, Fig. 1), even though their environmental conditions were not distinctive, suggesting potential synergies with ectomycorrhizal dominance (Brearley, 2012). Compositional shifts can also act to reduce differences in size-related distributions of biomass stocks and fluxes; for example, shifts towards more drought-tolerant species in drier sites may limit increases in mortality among large trees (Meakem *et al.*, 2018). These environmental factors should be evaluated in future studies encompassing more sites, ideally chosen along independent environmental and disturbance gradients to reduce confounding effects of multiple variables co-varying across sites.

Importance of small trees in AGB fluxes

Overall, relative aboveground woody productivity (RAWP) decreases across tree size classes, consistent with our expectations (Hypothesis 2a), with previous findings in tropical and temperate forests (Mencuccini *et al.*, 2005; Kohyama *et al.*, 2020), and with the expected decrease in photosynthetic activity (per unit mass; Poorter *et al.*, 2015a; Drake *et al.*, 2010) and increase in non-woody tissue investment (Ryan *et al.*, 2004; Thomas, 2011) as trees get larger. This pattern

was surprisingly similar across all our sites. This decrease in RAWP with size means that, consistent with our Hypothesis 2d, larger trees contribute less to AWP than to AGB, although they still dominate AWP and show higher absolute growth rates per individual tree (Muller-Landau *et al.*, 2006a; Stephenson *et al.*, 2014). In contrast, stems between 1 and 10 cm DBH – which are often omitted from forest inventories (e.g. Malhi *et al.*, 2002; Ploton *et al.*, 2020) – contribute more to AWP than to AGB (consistent with our Hypothesis 2c), with wide variation in proportional contributions among sites. While focusing on large trees has been suggested as an effective way of reducing sampling effort in forest inventories (Bastin *et al.*, 2018) and is the default for many remote sensing methods that can only measure canopy trees, it could result in biased estimation of forest biomass (and thus carbon) fluxes.

Synergies with vegetation demographic models

Dynamic global vegetation models integrated within Earth System models increasingly include explicit modeling of tree size distributions and demographic processes (Fisher *et al.*, 2018), presenting opportunities for synergies with empirical analyses of size-structured biomass dynamics. The results presented here provide valuable benchmarks to evaluate the performance of these models, especially with respect to size-structured biomass dynamics (Fisher *et al.*, 2018; Martínez Cano *et al.*, 2020). Vegetation demographic models can also be used to test mechanistic hypotheses for how potential drivers (climate, soil, stand age, disturbance regime) contribute to differences in observed tree size-related distributions of biomass stocks and fluxes. Comparative performance of different vegetation demographic model formulations against observed tree size distribution can provide insights into the relative importance of different processes in shaping size-related biomass dynamics (Longo *et al.*, 2019; Martínez Cano *et al.*, 2020; Koven *et al.*, 2020). For example, a study applying the vegetation demographic model FATES to BCI (Panama) found that FATES overpredicted the abundance of large trees and thus overestimated forest carbon stocks (Koven *et al.*, 2020). In contrast, a study applying the vegetation demographic model LM3PPA-TV, which incorporates branch turnover and hydraulic constraints on photosynthesis (unlike FATES) predicted a more realistic tree size distribution at BCI, as well as in eight other tropical forests (including 6 sites included in this study; Martínez Cano *et al.*, 2020).

In particular, among-site variation in size-related distributions of AWP and AWM may be explained in part by variation in how crown canopy position (e.g., emergent vs. canopy vs. understory) varies with diameter. After all, light availability and microclimate (e.g. wind speed, temperature, vapor pressure deficit) depend more on a tree's relative size and thus canopy position than on its absolute size (Stark *et al.*, 2012; Bachofen *et al.*, 2020; Zellweger *et al.*, 2020). Crown illumination or canopy position explains considerable variation in growth and survival among trees within sites, including on the BCI plot (Clark & Clark, 1992; Bohlman & Pacala, 2012). Among-site variation in how crown canopy position varies with tree size can itself be explained in large part by variation in tree size distributions, because the likelihood that a tree of a given size will be in the canopy depends on the abundance of larger trees. Vegetation demographic models seek to capture these patterns through algorithms that estimate light availability for trees as a function of local stand structure (Fisher *et al.*, 2018). These models have taken a variety of approaches to capturing size-specific AWP and AWM, from no redistribution of light between trees of different sizes, to perfect plasticity approximation approaches that fill successive tree crown layers from the top down and thus lead to much higher light availability for larger trees (Adams *et al.*, 2007). Our results on tree abundance and productivity by size class could be used to refine algorithms used to translate imposed vertical light distribution into modeled vegetation dynamics, with the goal of comparing the potential of different algorithms to capture observed AGB, AWP and AWM patterns.

Sources of uncertainty

Size-specific patterns of AWP and AWM are variable over time within sites. This is especially true for AWM that has a much larger sampling error and temporal variation than AWP and AGB (Muller-Landau *et al.*, 2021), which may explain why there were fewer significant effects of climate on AWM in our analyses. Climate variation and periodic disturbances, such as El Niño events, can alter size-structured mortality and productivity patterns (Meakem *et al.*, 2018). For example, the low mortality of small stems observed in Zofin can be largely attributed to the recovery from two winter windstorms in 2007 and 2008 that created large gaps in the canopy and thus increased productivity and decreased mortality of small stems (Janík *et al.*, 2018). Analyses such as ours that rely on a single 5-10 year time period may not adequately represent long-term averages, nor the shorter-term responses to weather events such as wind storms or droughts. In

addition to increasing the frequency and number of censuses, pairing census data with analyses of the differential climate sensitivities of large and small trees derived from tree-ring analyses (e.g., McGregor *et al.*, 2021) or long-term dendrometer band records could reveal how forest productivity and its size structure vary in response to climatic differences. Furthermore, combining such analyses with mechanistic modeling could enable us to test the effects of multiple environmental drivers on the distribution of biomass stocks and fluxes with tree size.

One major source of uncertainty in the patterns shown here derives from biomass allometries. AGB, AWP, AWM were all calculated from generalized AGB allometric equations that fail to fully capture among-site (and within-site) variation (Ngomanda *et al.*, 2014). Moreover, large trees are usually undersampled in biomass allometric equations, increasing errors in estimates of their contributions (Disney *et al.*, 2020; Burt *et al.*, 2020). A crucial step for future research is to improve the accuracy of allometric equations across tree size classes and forests, or to get beyond the use of allometric equations altogether by developing other direct forest biomass estimation methods. One promising approach involves recently developed methods to nondestructively estimate tree woody volume, a good proxy for biomass, from terrestrial LiDAR (Disney, 2019; Stovall *et al.*, 2018).

Future directions

Future work should expand on the results presented here by assessing how other carbon stocks and fluxes are distributed with tree size. Our analysis focuses on estimated AGB, the largest and longest-lived tree carbon pool, but not the only one of interest. Leaves, reproductive organs, and roots are responsible for a large proportion of NPP (Malhi *et al.*, 2011; Anderson-Teixeira *et al.*, 2021), and allocation of carbon to these organs varies with ontogeny and tree size. For example, large trees allocate a larger proportion of their resources to reproduction than small trees (Thomas, 2011). In contrast, small trees allocate a greater proportion of their carbon to roots than large trees (Ledo *et al.*, 2018). Further, our analysis of woody productivity encompasses only net increases in biomass of trees as estimated from their diameter, missing the woody productivity associated with branch turnover. Branchfall contributes to a large proportion of woody turnover (Ouimette *et al.*, 2018; Marvin & Asner, 2016), and branch loss is expected to be higher for large senescent trees (Jans *et al.*, 1993), which may moderate the lower contribution of large trees to AWP than AGB. Correctly accounting for allocation to branch turnover is critical to obtaining

accurate stand-level forest dynamics in vegetation models (Martínez Cano *et al.*, 2020) but this is difficult and no data are available for our forest plots.

Looking forward, a key question is how climate change will alter forest biomass stocks and fluxes and their distribution across tree size. The frequency and intensity of extreme climatic events such as droughts, floods, lightning strikes and cyclones are expected to increase in the future (Differbaugh *et al.*, 2017; Marsooli *et al.*, 2019). These disturbances will likely increase the mortality of large canopy trees (and of understory trees that large trees damage when they fall) because large trees are more vulnerable to water stress (Bennett *et al.*, 2015), more exposed to lightning (Gora *et al.*, 2020) and have lower mechanical stability (James *et al.*, 2006). Lower abundance of large trees after disturbance in turn increases understory light availability, and the number and woody productivity of smaller trees (Hogan *et al.*, 2016). However, the effect of increased light availability on the productivity of small trees adapted to dense forest microclimates may be limited by more variable precipitation regimes, and higher temperatures that increase evaporative demand (Elliott *et al.*, 2015; Germain & Lutz, 2020; Konapala *et al.*, 2020; Smith *et al.*, 2020; Muller-Landau *et al.*, 2021). More research is needed to understand how forest tree size structure and biomass dynamics are related to climate, and in turn how forest dynamics will respond to global climate change. In providing the first global-scale analysis of tree size structuring of biomass dynamics in forests, our analyses set a foundation for building better climate models and understanding the interactions between forests and future climate change.

Acknowledgements

CP was supported by the ForestGEO network of the Smithsonian Tropical Research Institute. We thank all technicians, volunteers and students who participated in field data collection.

Acknowledgments for the support that the 25 sites included in this study received are provided in the Supporting information, Notes S2.

Author contributions

CP, KJA-T and HCM-L designed the research. CP carried out the data analysis, under guidance of HCM-L and KJA-T. CP, HCM-L and KJA-T interpreted the results. All coauthors (except CP)

participated in data collection. CP wrote the manuscript, with the help of HCM-L and KJA-T. The manuscript was reviewed by all coauthors.

Data availability

Data for plots in the ForestGEO network are available through the online portal at: <http://www.forestgeo.si.edu>. Aggregated data used in this study are provided in the Supporting information (Datasets S1, S2, S3).

References

- Adams TP, Purves DW, Pacala SW. 2007.** Understanding height-structured competition in forests: is there an R * for light? *Proceedings of the Royal Society B: Biological Sciences* **274**: 3039–3048.
- Anderson-Teixeira KJ, Davies SJ, Bennett AC, Gonzalez-Akre EB, Muller-Landau HC, Joseph Wright S, Abu Salim K, Almeyda Zambrano AM, Alonso A, Baltzer JL et al. 2015a.** CTFS-ForestGEO: A worldwide network monitoring forests in an era of global change. *Global Change Biology* **21**: 528–549.
- Anderson-Teixeira KJ, Herrmann V, Banbury Morgan R, Bond-Lamberty B, Cook-Patton SC, Ferson AE, Muller-Landau HC, Wang MMH. 2021.** Carbon cycling in mature and regrowth forests globally. *Environmental Research Letters* **16**: 053009.
- Anderson-Teixeira KJ, McGarvey JC, Muller-Landau HC, Park JY, Gonzalez-Akre EB, Herrmann V, Bennett AC, So CV, Bourg NA, Thompson JR et al. 2015b.** Size-related scaling of tree form and function in a mixed-age forest. *Functional Ecology* **29**: 1587–1602.
- Bachofen C, D’Odorico P, Buchmann N. 2020.** Light and VPD gradients drive foliar nitrogen partitioning and photosynthesis in the canopy of European beech and silver fir. *Oecologia* **192**: 323–339.
- Banbury Morgan R, Herrmann V, Kunert N, Bond-Lamberty B, Muller-Landau HC, Anderson-Teixeira KJ. 2021.** Global patterns of forest autotrophic carbon fluxes. *Global Change Biology* **27**: 2840–2855.

- Bastin J-F, Rutishauser E, Kellner JR, Saatchi S, Péliissier R, Hérault B, Slik F, Bogaert J, De Cannière C, Marshall AR et al. 2018.** Pan-tropical prediction of forest structure from the largest trees. *Global Ecology and Biogeography* **27**: 1366–1383.
- Bennett AC, McDowell NG, Allen CD, Anderson-Teixeira KJ. 2015.** Larger trees suffer most during drought in forests worldwide. *Nature Plants* **1**: 15139.
- Bohlman S, Pacala S. 2012.** A forest structure model that determines crown layers and partitions growth and mortality rates for landscape-scale applications of tropical forests. *Journal of Ecology* **100**: 508–518.
- Brando PM, Nepstad DC, Balch JK, Bolker B, Christman MC, Coe M, Putz FE. 2012.** Fire-induced tree mortality in a neotropical forest: The roles of bark traits, tree size, wood density and fire behavior. *Global Change Biology* **18**: 630–641.
- Brearley FQ. 2012.** Ectomycorrhizal Associations of the Dipterocarpaceae. *Biotropica* **44**: 637–648.
- Burt A, Calders K, Cuni-Sanchez A, Gómez-Dans J, Lewis P, Lewis SL, Malhi Y, Phillips OL, Disney M. 2020.** Assessment of Bias in Pan-Tropical Biomass Predictions. *Frontiers in Forests and Global Change* **3**: Article 12.
- Chave J, Réjou-Méchain M, Burquez A, Chidumayo E, Colgan MS, Delitti WBC, Duque A, Eid T, Fearnside PM, Goodman RC et al. 2014.** Improved allometric models to estimate the aboveground biomass of tropical trees. *Global Change Biology* **20**: 3177–3190.
- Chojnacky DC, Heath LS, Jenkins JC. 2014.** Updated generalized biomass equations for North American tree species. *Forestry* **87**: 129–151.
- Clark DA, Clark DB. 1992.** Life History Diversity of Canopy and Emergent Trees in a Neotropical Rain Forest. *Ecological Monographs* **62**: 315.
- Coley PD. 1988.** Effects of plant growth rate and leaf lifetime on the amount and type of anti-herbivore defense. *Oecologia* **74**: 531–536.
- Condit RS. 1998.** *Tropical forest census plots: methods and results from Barro Colorado Island, Panama and a comparison with other plots*. Berlin, Germany: Springer-Verlag.

- Côté SD, Rooney TP, Tremblay J-P, Dussault C, Waller DM. 2004.** Ecological Impacts of Deer Overabundance. *Annual Review of Ecology, Evolution, and Systematics* **35**: 113–147.
- Cushman KC, Bunyavejchewin S, Cárdenas D, Condit R, Davies SJ, Duque Á, Hubbell SP, Kiratiprayoon S, Lum SKY, Muller-Landau HC. 2021.** Variation in trunk taper of buttressed trees within and among five lowland tropical forests. *Biotropica* **53**: 1442–1453.
- Davies SJ, Abiem I, Abu Salim K, Aguilar S, Allen D, Alonso A, Anderson-Teixeira K, Andrade A, Arellano G, Ashton PS et al. 2021.** ForestGEO: Understanding forest diversity and dynamics through a global observatory network. *Biological Conservation* **253**: 108907.
- Diffenbaugh NS, Singh D, Mankin JS, Horton DE, Swain DL, Touma D, Charland A, Liu Y, Haugen M, Tsiang M et al. 2017.** Quantifying the influence of global warming on unprecedented extreme climate events. *Proceedings of the National Academy of Sciences of the United States of America* **114**: 4881–4886.
- Disney M. 2019.** Terrestrial LiDAR: a three-dimensional revolution in how we look at trees. *New Phytologist* **222**: 1736–1741.
- Disney M, Burt A, Wilkes P, Armston J, Duncanson L. 2020.** New 3D measurements of large redwood trees for biomass and structure. *Scientific Reports* **10**: 1–11.
- Drake JE, Raetz LM, Davis SC, Delucia EH. 2010.** Hydraulic limitation not declining nitrogen availability causes the age-related photosynthetic decline in loblolly pine (*Pinus taeda* L.). *Plant, Cell and Environment* **33**: 1756–1766.
- Elliott KJ, Miniati CF, Pederson N, Laseter SH. 2015.** Forest tree growth response to hydroclimate variability in the southern Appalachians. *Global Change Biology* **21**: 4627–4641.
- Estes JA, Terborgh J, Brashares JS, Power ME, Berger J, Bond WJ, Carpenter SR, Essington TE, Holt RD, Jackson JBC et al. 2011.** Trophic downgrading of planet earth. *Science* **333**: 301–306.
- Fisher RA, Koven CD, Anderegg WRL, Christoffersen BO, Dietze MC, Farrior CE, Holm JA, Hurtt GC, Knox RG, Lawrence PJ et al. 2018.** Vegetation demographics in Earth System Models: A review of progress and priorities. *Global Change Biology* **24**: 35–54.

- Gardiner B, Marshall B, Achim A, Belcher R, Wood C. 2005.** The stability of different silvicultural systems: a wind-tunnel investigation. *Forestry: An International Journal of Forest Research* **78**: 471–484.
- Germain SJ, Lutz JA. 2020.** Climate extremes may be more important than climate means when predicting species range shifts. *Climatic Change* **163**: 579–598.
- Gora EM, Esquivel-Muelbert A. 2021.** Implications of size-dependent tree mortality for tropical forest carbon dynamics. *Nature Plants* **7**: 384–391.
- Gora EM, Muller-Landau HC, Burchfield JC, Bitzer PM, Hubbell SP, Yanoviak SP. 2020.** A mechanistic and empirically supported lightning risk model for forest trees. *Journal of Ecology* **108**: 1956–1966.
- Hogan JA, Zimmerman JK, Thompson J, Nytch CJ, Uriarte M. 2016.** The interaction of land-use legacies and hurricane disturbance in subtropical wet forest: Twenty-one years of change. *Ecosphere* **7**: 1–18.
- Hood SM, Varner JM, Mantgem P van, Cansler CA. 2018.** Fire and tree death: understanding and improving modeling of fire-induced tree mortality. *Environmental Research Letters* **13**: 113004.
- Hubau W, De Mil T, Van den Bulcke J, Phillips OL, Angoboy Ilondea B, Van Acker J, Sullivan MJP, Nsenga L, Toirambe B, Couralet C *et al.* 2019.** The persistence of carbon in the African forest understory. *Nature Plants* **5**: 133–140.
- James KR, Haritos N, Ades PK. 2006.** Mechanical stability of trees under dynamic loads. *American Journal of Botany* **93**: 1522–1530.
- Janík D, Vrška T, Hort L, Unar P, Král K. 2018.** Where have all the tree diameters grown? Patterns in *Fagus sylvatica* L. diameter growth on their run to the upper canopy. *Ecosphere* **9**: e02508.
- Jans L, Poorter L, Rompaey RSAR van, Bongers F. 1993.** Gaps and Forest Zones in Tropical Moist Forest in Ivory Coast. *Biotropica* **25**: 258–269.

Karger DN, Conrad O, Böhner J, Kawohl T, Kreft H, Soria-Auza RW, Zimmermann NE, Linder HP, Kessler M. 2017. Climatologies at high resolution for the earth's land surface areas. *Scientific Data* **4**: 1–20.

King DA, Davies SJ, Noor NSM. 2006. Growth and mortality are related to adult tree size in a Malaysian mixed dipterocarp forest. *Forest Ecology and Management* **223**: 152–158.

Koch GW, Sillett SC, Jennings GM, Davis SD. 2004. The limits to tree height. *Nature* **428**: 851–854.

Kohyama TS, Kohyama TI, Sheil D. 2019. Estimating net biomass production and loss from repeated measurements of trees in forests and woodlands: Formulae, biases and recommendations. *Forest Ecology and Management* **433**: 729–740.

Kohyama TS, Potts MD, Kohyama TI, Niiyama K, Yao TL, Davies SJ, Sheil D. 2020. Trade-off between standing biomass and productivity in species-rich tropical forest: Evidence, explanations and implications (G Zotz, Ed.). *Journal of Ecology* **108**: 2571–2583.

Konapala G, Mishra AK, Wada Y, Mann ME. 2020. Climate change will affect global water availability through compounding changes in seasonal precipitation and evaporation. *Nature Communications* **11**: 1–10.

Koven CD, Knox RG, Fisher RA, Chambers JQ, Christoffersen BO, Davies SJ, Detto M, Dietze MC, Faybishenko B, Holm J *et al.* 2020. Benchmarking and parameter sensitivity of physiological and vegetation dynamics using the Functionally Assembled Terrestrial Ecosystem Simulator (FATES) at Barro Colorado Island, Panama. *Biogeosciences* **17**: 3017–3044.

Ledo A, Paul KI, Burslem DFRP, Ewel JJ, Barton C, Battaglia M, Brooksbank K, Carter J, Eid TH, England JR *et al.* 2018. Tree size and climatic water deficit control root to shoot ratio in individual trees globally. *New Phytologist* **217**: 8–11.

Lewis SL, Edwards DP, Galbraith D. 2015. Increasing human dominance of tropical forests. *Science* **349**: 827–832.

Longo M, Knox RG, Medvigy DM, Levine NM, Dietze MC, Kim Y, Swann ALS, Zhang K, Rollinson CR, Bras RL *et al.* 2019. The biophysics, ecology, and biogeochemistry of functionally diverse, vertically and horizontally heterogeneous ecosystems: The Ecosystem

Demography model, version 2.2-Part 1: Model description. *Geoscientific Model Development* **12**: 4309–4346.

Lutz JA, Furniss TJ, Johnson DJ, Davies SJ, Allen D, Alonso A, Anderson-Teixeira KJ, Andrade A, Baltzer J, Becker KMLL et al. 2018. Global importance of large-diameter trees. *Global Ecology and Biogeography* **27**: 849–864.

Magnani F, Mencuccini M, Grace J. 2000. Age-related decline in stand productivity: The role of structural acclimation under hydraulic constraints. *Plant, Cell and Environment* **23**: 251–263.

Malhi Y, Doughty C, Galbraith D. 2011. The allocation of ecosystem net primary productivity in tropical forests. *Philosophical Transactions of the Royal Society B: Biological Sciences* **366**: 3225–3245.

Malhi Y, Phillips OL, Lloyd J, Baker T, Wright J, Almeida S, Arroyo L, Frederiksen T, Grace J, Higuchi N et al. 2002. An international network to monitor the structure, composition and dynamics of Amazonian forests (RAINFOR). *Journal of Vegetation Science* **13**: 439–450.

Marsooli R, Lin N, Emanuel K, Feng K. 2019. Climate change exacerbates hurricane flood hazards along US Atlantic and Gulf Coasts in spatially varying patterns. *Nature Communications* **10**: 1–9.

Martínez Cano I, Shevliakova E, Malyshev S, Wright SJ, Detto M, Pacala SW, Muller-Landau HC. 2020. Allometric constraints and competition enable the simulation of size structure and carbon fluxes in a dynamic vegetation model of tropical forests (LM3PPA-TV). *Global Change Biology* **26**: 4478–4494.

Marvin DC, Asner GP. 2016. Branchfall dominates annual carbon flux across lowland Amazonian forests. *Environmental Research Letters* **11**: 094027.

McDowell N, Allen CD, Anderson-Teixeira K, Brando P, Brienen R, Chambers J, Christoffersen B, Davies S, Doughty C, Duque A et al. 2018. Drivers and mechanisms of tree mortality in moist tropical forests. *New Phytologist* **219**: 851–869.

McEwan RW, Lin YC, Sun IF, Hsieh CF, Su SH, Chang LW, Song GZM, Wang HH, Hwong JL, Lin KC et al. 2011. Topographic and biotic regulation of aboveground carbon storage in subtropical broad-leaved forests of Taiwan. *Forest Ecology and Management* **262**: 1817–1825.

McGarvey JC, Bourg NA, Thompson JR, McShea WJ, Shen X. 2013. Effects of Twenty Years of Deer Exclusion on Woody Vegetation at Three Life-History Stages in a Mid-Atlantic Temperate Deciduous Forest. *Northeastern Naturalist* **20**: 451–468.

McGregor IR, Helcoski R, Kunert N, Tepley AJ, Gonzalez-Akre EB, Herrmann V, Zailaa J, Stovall AEL, Bourg NA, McShea WJ et al. 2021. Tree height and leaf drought tolerance traits shape growth responses across droughts in a temperate broadleaf forest. *New Phytologist* **231**: 601–616.

Meakem V, Tepley AJ, Gonzalez-Akre EB, Herrmann V, Muller-Landau HC, Wright SJ, Hubbell SP, Condit R, Anderson-Teixeira KJ. 2018. Role of tree size in moist tropical forest carbon cycling and water deficit responses. *New Phytologist* **219**: 947–958.

Meer PJ van der, Bongers F. 1996. Patterns of Tree-Fall and Branch-Fall in a Tropical Rain Forest in French Guiana. *Journal of Ecology* **84**: 19–29.

Mencuccini M, Martínez-Vilalta J, Vanderklein D, Hamid HA, Korakaki E, Lee S, Michiels B. 2005. Size-mediated ageing reduces vigour in trees. *Ecology Letters* **8**: 1183–1190.

Mensah S, Noulékoun F, Ago EE. 2020. Aboveground tree carbon stocks in West African semi-arid ecosystems: Dominance patterns, size class allocation and structural drivers. *Global Ecology and Conservation* **24**: e01331.

Mildrexler DJ, Berner LT, Law BE, Birdsey RA, Moomaw WR. 2020. Large Trees Dominate Carbon Storage in Forests East of the Cascade Crest in the United States Pacific Northwest. *Frontiers in Forests and Global Change* **3**: 1–15.

Muller-Landau HC, Condit RS, Chave J, Thomas SC, Bohlman SA, Bunyavejchewin S, Davies S, Foster R, Gunatilleke S, Gunatilleke N et al. 2006a. Testing metabolic ecology theory for allometric scaling of tree size, growth and mortality in tropical forests. *Ecology Letters* **9**: 575–588.

Muller-Landau HC, Condit RS, Harms KE, Marks CO, Thomas SC, Bunyavejchewin S, Chuyong G, Co L, Davies S, Foster R et al. 2006b. Comparing tropical forest tree size distributions with the predictions of metabolic ecology and equilibrium models. *Ecology Letters* **9**: 589–602.

- Muller-Landau HC, Cushman KC, Arroyo EE, Martinez Cano I, Anderson-Teixeira KJ, Backiel B. 2021.** Patterns and mechanisms of spatial variation in tropical forest productivity, woody residence time, and biomass. *New Phytologist* **229**: 3065–3087.
- Newbery DM, Van Der Burgt XM, Worbes M, Chuyong GB. 2013.** Transient dominance in a central african rain forest. *Ecological Monographs* **83**: 339–382.
- Ngomanda A, Engone Obiang NL, Lebamba J, Moundounga Mavouroulou Q, Gomat H, Mankou GS, Loumeto J, Midoko Iponga D, Kossi Ditsouga F, Zinga Koumba R et al. 2014.** Site-specific versus pantropical allometric equations: Which option to estimate the biomass of a moist central African forest? *Forest Ecology and Management* **312**: 1–9.
- Ouimette AP, Ollinger SV, Richardson AD, Hollinger DY, Keenan TF, Lepine LC, Vadeboncoeur MA. 2018.** Carbon fluxes and interannual drivers in a temperate forest ecosystem assessed through comparison of top-down and bottom-up approaches. *Agricultural and Forest Meteorology* **256-257**: 420–430.
- Pfeifer EM, Hicke JA, Meddens AJH. 2011.** Observations and modeling of aboveground tree carbon stocks and fluxes following a bark beetle outbreak in the western United States. *Global Change Biology* **17**: 339–350.
- Ploton P, Mortier F, Barbier N, Cornu G, Réjou-Méchain M, Rossi V, Alonso A, Bastin J-f, Bayol N, Bénédet F et al. 2020.** A map of African humid tropical forest aboveground biomass derived from management inventories. *Scientific Data* **7**: 221.
- Poorter H, Jagodzinski AM, Ruiz-Peinado R, Kuyah S, Luo Y, Oleksyn J, Usoltsev VA, Buckley TN, Reich PB, Sack L. 2015a.** How does biomass distribution change with size and differ among species? An analysis for 1200 plant species from five continents. *New Phytologist* **208**: 736–749.
- Poorter L, Sande MT van der, Thompson J, Arets EJMM, Alarcón A, Álvarez-Sánchez J, Ascarrunz N, Balvanera P, Barajas-Guzmán G, Boit A et al. 2015b.** Diversity enhances carbon storage in tropical forests. *Global Ecology and Biogeography* **24**: 1314–1328.
- Quesada Ca, Phillips OL, Schwarz M, Czimczik CI, Baker TR, Patiño S, Fyllas NM, Hodnett MG, Herrera R, Almeida S et al. 2012.** Basin-wide variations in Amazon forest structure and function are mediated by both soils and climate. *Biogeosciences* **9**: 2203–2246.

- Réjou-Méchain M, Tanguy A, Piponiot C, Chave J, Hérault B. 2017.** BIOMASS: An R Package for estimating above-ground biomass and its uncertainty in tropical forests (S Goslee, Ed.). *Methods in Ecology and Evolution* **8**: 1163–1167.
- Ryan MG, Binkley D, Fownes JH, Giardina CP, Senock RS. 2004.** An experimental test of the causes of forest growth decline with stand age. *Ecological Monographs* **74**: 393–414.
- Segura G, Balvanera P, Durán E, Pérez A. 2002.** Tree community structure and stem mortality along a water availability gradient in a Mexican tropical dry forest. *Plant Ecology* **169**: 259–271.
- Seidl R, Thom D, Kautz M, Martin-Benito D, Peltoniemi M, Vacchiano G, Wild J, Ascoli D, Petr M, Honkaniemi J et al. 2017.** Forest disturbances under climate change. *Nature Climate Change* **7**: 395–402.
- Slik JWF, Paoli G, McGuire K, Amaral I, Barroso J, Bastian M, Blanc L, Bongers F, Boundja P, Clark C et al. 2013.** Large trees drive forest aboveground biomass variation in moist lowland forests across the tropics. *Global Ecology and Biogeography* **22**: 1261–1271.
- Smith MN, Taylor TC, Haren J van, Rosolem R, Restrepo-Coupe N, Adams J, Wu J, Oliveira RC de, Silva R da, Araujo AC de et al. 2020.** Empirical evidence for resilience of tropical forest photosynthesis in a warmer world. *Nature Plants* **6**: 1225–1230.
- Stark SC, Enquist BJ, Saleska SR, Leitold V, Schiatti J, Longo M, Alves LF, Camargo PB, Oliveira RC. 2015.** Linking canopy leaf area and light environments with tree size distributions to explain Amazon forest demography. *Ecology Letters* **18**: 636–645.
- Stark SC, Leitold V, Wu JL, Hunter MO, Castilho CV de, Costa FRC, McMahon SM, Parker GG, Shimabukuro MT, Lefsky MA et al. 2012.** Amazon forest carbon dynamics predicted by profiles of canopy leaf area and light environment. *Ecology Letters* **15**: 1406–1414.
- Stephenson NL, Das AJ, Condit R, Russo SE, Baker PJ, Beckman NG, Coomes DA, Lines ER, Morris WK, Rüger N et al. 2014.** Rate of tree carbon accumulation increases continuously with tree size. *Nature* **507**: 90–93.
- Stovall AEL, Anderson-Teixeira KJ, Shugart HH. 2018.** Assessing terrestrial laser scanning for developing non-destructive biomass allometry. *Forest Ecology and Management* **427**: 217–229.

Thomas SC. 2011. Age-Related Changes in Tree Growth and Functional Biology: The Role of Reproduction. In: Meinzer FC, In: Lachenbruch B, In: Dawson TE, eds. Size- and age-related changes in tree structure and function. Dordrecht, Netherlands: Springer Netherlands, 33–64.

Valladares F, Niinemets Ü. 2008. Shade tolerance, a key plant feature of complex nature and consequences. *Annual Review of Ecology, Evolution, and Systematics* **39**: 237–257.

Vincent JB, Turner BL, Alok C, Novotny V, Weiblen GD, Whitfeld TJS. 2018. Tropical forest dynamics in unstable terrain: A case study from New Guinea. *Journal of Tropical Ecology* **34**: 157–175.

Yanoviak SP, Gora EM, Bitzer PM, Burchfield JC, Muller-Landau HC, Detto M, Paton S, Hubbell SP. 2020. Lightning is a major cause of large tree mortality in a lowland neotropical forest. *New Phytologist* **225**: 1936–1944.

Zanne AE, Lopez-Gonzalez G, Coomes DAA, Ilic J, Jansen S, Lewis SLSL, Miller RBB, Swenson NGG, Wiemann MCC, Chave J. 2009. Global wood density database, <https://doi.org/10.5061/dryad.234>.

Zellweger F, De Frenne P, Lenoir J, Vangansbeke P, Verheyen K, Bernhardt-Römermann M, Baeten L, Hédli R, Berki I, Brunet J *et al.* 2020. Forest microclimate dynamics drive plant responses to warming. *Science* **368**: 772–775.

Zuidema PA, Baker PJ, Groenendijk P, Schippers P, Sleen P van der, Vlam M, Sterck F. 2013. Tropical forests and global change: Filling knowledge gaps. *Trends in Plant Science* **18**: 413–419.

Supporting information

Fig. S1: Location and environmental conditions of study sites.

Fig. S2: Distribution of modulus-transformed DBH growth values from individual trees in the BCI data as an example.

Fig. S3: Distribution of modulus-transformed DBH growth values from individual trees in five different sites.

Fig. S4: Definition of diameter classes per site.

Fig. S5: Proportions of AGB stocks and fluxes in large trees, when defined as the 5% largest stems in each site.

Fig. S6: Proportions of AGB stocks and fluxes in large trees, when defined as the largest trees comprising 50% of total AGB in each site.

Fig. S7: Size-related variation in stem density, mean individual stem aboveground biomass, and total aboveground live biomass.

Fig. S8: Size-related variation in mean stem diameter growth and total aboveground woody productivity.

Fig. S9: Size-related variation in stem mortality rate and total aboveground woody mortality.

Fig. S10: Size-related distribution of AGB stocks and fluxes per site.

Fig. S11: Untruncated Fig. 1.

Fig. S12: Untruncated Fig. 4.

Table S1: Plot initiation papers.

Table S2: Disturbances at ForestGEO sites used in this study.

Table S3: Total number of diameter classes per site.

Table S4: Estimated effects of the multiple linear regressions of the median and skewness with mean annual temperature and precipitation.

Table S5: Estimated effects of the multiple linear regressions of the median, dispersion and skewness with mean annual temperature and SHC (moisture index).

Table S6: Wilcoxon signed-rank tests results comparing the median, dispersion and skewness of size-related distributions in tropical vs temperate forests.

Table S7: DBH threshold per site for the alternative definitions of large trees.

Methods S1: Methods for calculating instantaneous biomass fluxes

Methods S2: Methods for gap-filling DBH growth

Methods S3: Definition of diameter classes for graphing

Notes S1: Description of additional variables

Notes S2: Site-specific acknowledgments

Dataset S1: Total AGB, AWP, and AWM for each site and site-specific diameter classes (in cm), as presented in the figures.

Dataset S2: Total AGB, AWP, and AWM for each site by standardized diameter classes of [1,5), [5,10), [10,20), [20,30), [30,40), [40,50), [50,100), [100,200), and [200, + ∞) cm DBH.

Dataset S3: Median, dispersion and skewness of AGB, AWP and AWM distributions at each site.

Table 1 Characteristics and mean woody aboveground biomass carbon stocks and fluxes of the focal ForestGEO plots and census intervals.

Site	Code	Lat.	Long.	MAP (mm)	MAT (°C)	Area (ha)	Census period	AGB (Mg ha ⁻¹)	AWP (Mg ha ⁻¹ yr ⁻¹)	AWM (Mg ha ⁻¹ yr ⁻¹)
Lenda	LE	1.315	28.65	1682	24.3	20.0	2001-2007	482 (460-504)	5.19 (4.94-5.49)	6.72 (5.21-8.33)
Edoro	ED	1.560	28.52	1682	24.3	20.0	2001-2007	353 (335-372)	5.23 (4.99-5.55)	3.94 (3.05-4.93)
Pasoh	PS	2.980	102.31	1788	27.9	50.0	2005-2010	321 (309-334)	8.27 (8.04-8.53)	9.58 (8.46-10.9)

Amacayacu	AM	-3.810	-70.27	3215	25.8	25.0	2007-2016	288 (277-299)	4.14 (3.92-4.36)	5.62 (5.07-6.19)
Lambir	LM	4.190	114.02	2664	26.6	52.0	2003-2008	518 (501-534)	8.58 (8.37-8.82)	6.57 (5.79-7.45)
Korup	KO	5.070	8.85	5272	26.6	50.0	1997-2009	362 (342-382)	4.29 (4.03-4.54)	5.87 (5-6.79)
Danum Valley	DA	5.100	117.69	2822	26.7	50.0	2011-2019	342 (325-360)	10.8 (10.3-11.2)	6.99 (5.73-8.5)
Wanang	WG	-5.250	145.27	3500	26.0	50.0	2010-2017	317 (302-334)	7.76 (7.44-8.12)	10.2 (8.88-11.6)
Sinharaja	SI	6.400	80.40	5016	22.5	25.0	2001-2008	530 (502-559)	9.03 (8.57-9.51)	10.8 (8.98-12.6)
Cocoli	CO	8.990	-79.62	1950	26.6	4.0	1994-1997	281 (242-321)	6.95 (5.76-8.06)	2.61 (1.34-4.37)
BCI	BC	9.150	-79.85	2551	27.1	50.0	2010-2015	288 (276-303)	6.45 (6.23-6.69)	6.64 (6.01-7.38)
San Lorenzo	SL	9.280	-79.97	3030	26.2	6.0	1999-2009	303 (271-334)	5.64 (4.99-6.3)	6.77 (5.21-8.73)
Mudumalai	MU	11.600	76.53	1255	22.7	50.0	1996-2000	225 (219-231)	4.03 (3.9-4.17)	1.44 (1.18-1.77)
Luquillo	LU	18.330	-65.82	3548	22.8	16.0	2011-2016	312 (298-328)	4.2 (4.02-4.39)	4.21 (3.68-4.75)

Palamanui	PL	19.740	- 155.99	835	20.0	4.0	2008- 2014	42.1 (37.4- 46.8)	0.454 (0.407- 0.498)	0.729 (0.441- 1.14)
Laupahoehoe	LP	19.930	- 155.29	3440	16.0	4.0	2008- 2013	414 (366- 464)	12.3 (11- 13.6)	3.81 (1.98- 6.2)
Fushan	FU	24.760	121.56	4271	18.2	25.0	2008- 2013	202 (195- 209)	4.84 (4.67- 5.02)	2.4 (2.15- 2.69)
Gutianshan	GU	29.250	118.12	1964	15.3	24.0	2010- 2015	225 (218- 233)	5.14 (4.95- 5.35)	5.73 (5.38- 6.1)
SCBI	SC	38.890	-78.15	1001	12.9	25.6	2013- 2018	279 (268- 290)	4.93 (4.74- 5.14)	3.12 (2.61- 3.66)
SERC	SE	38.890	-76.56	1068	13.2	16.0	2008- 2014	273 (253- 293)	3.58 (3.28- 3.87)	2.65 (1.8- 3.74)
Changbaishan	CB	42.380	128.08	700	2.9	25.0	2004- 2009	302 (294- 311)	3.55 (3.37- 3.72)	1.79 (1.39- 2.27)
MBW	MB	42.470	-84.00	857	8.6	23.0	2007- 2014	211 (201- 221)	4.7 (4.5- 4.88)	1.82 (1.46- 2.22)
Wabikon	WK	45.550	-88.79	805	4.2	25.2	2013- 2018	173 (169- 178)	3.59 (3.48- 3.71)	1.66 (1.43- 1.9)
Wind River	WR	45.820	- 121.96	2495	9.2	27.2	2011- 2016	503 (480- 530)	3.1 (2.95- 3.24)	5.04 (3.98- 6.15)
Zofin	ZO	48.660	14.71	866	6.2	25.0	2012- 2017	300 (285- 315)	6.54 (6.19- 6.9)	3.07 (2.2- 4.02)

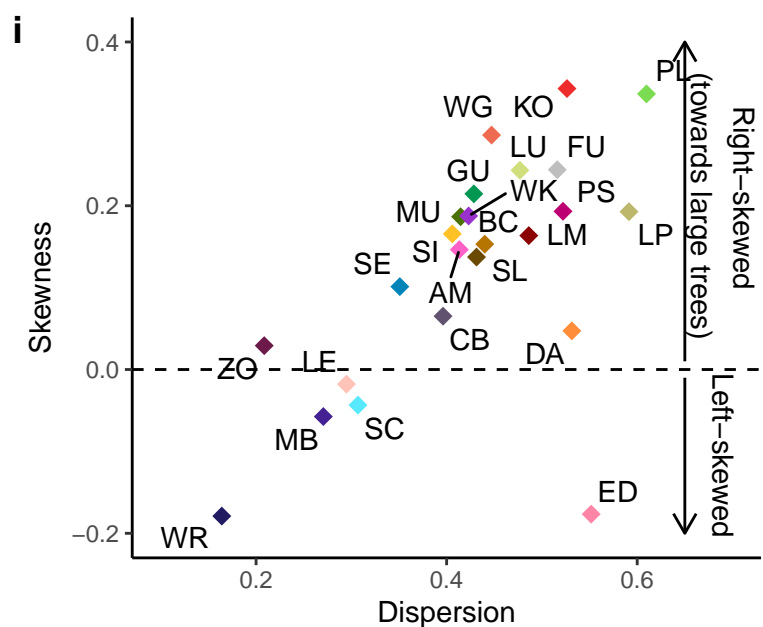
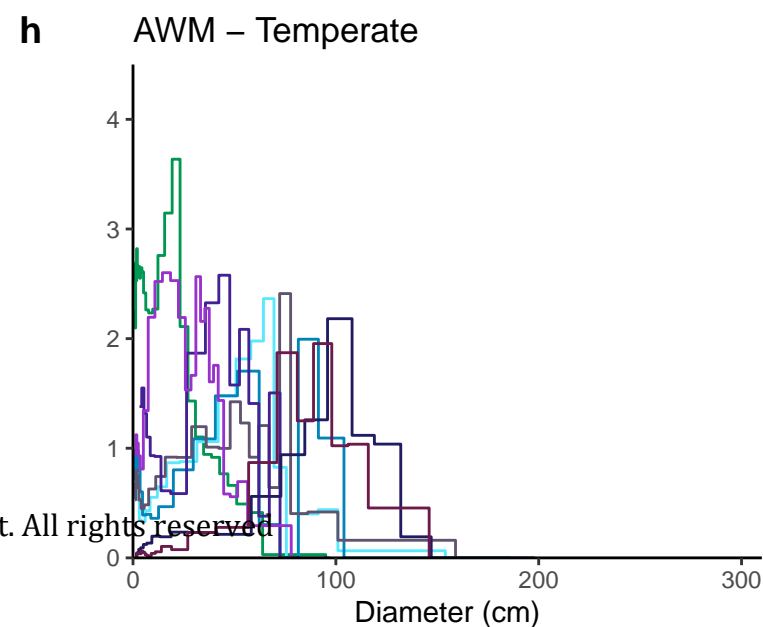
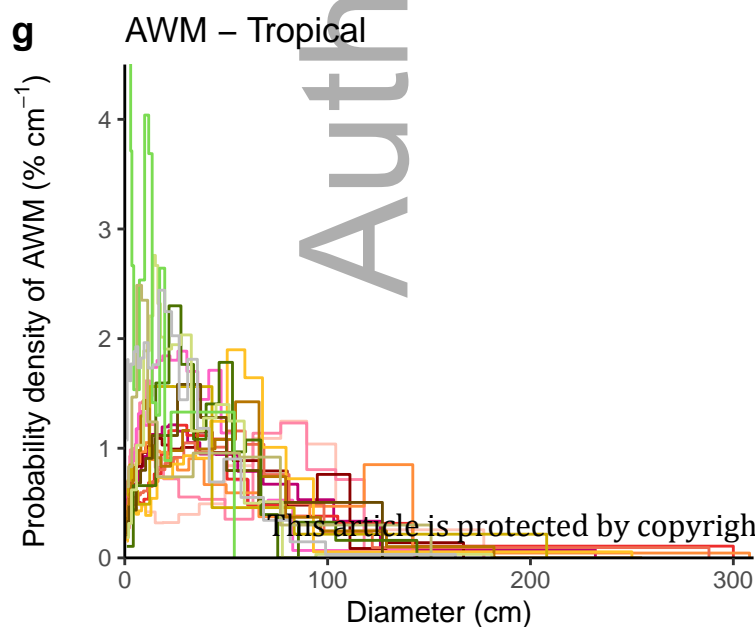
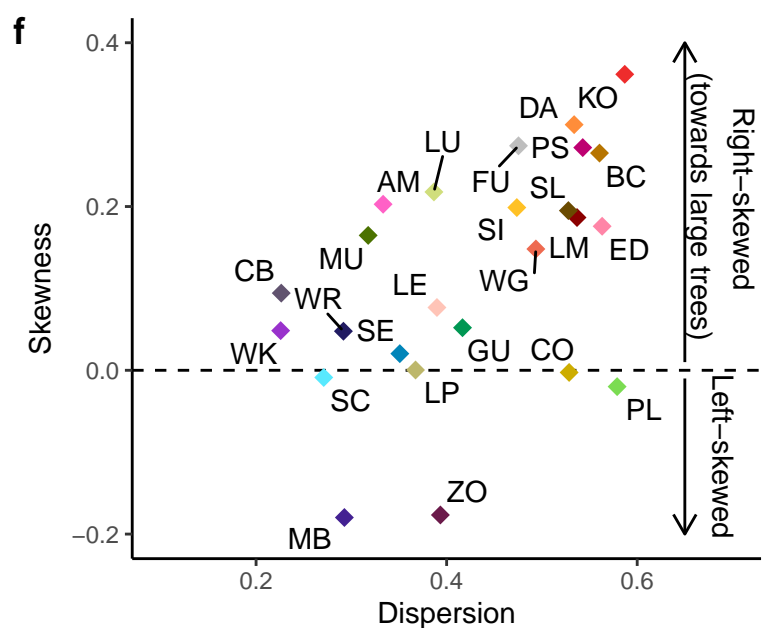
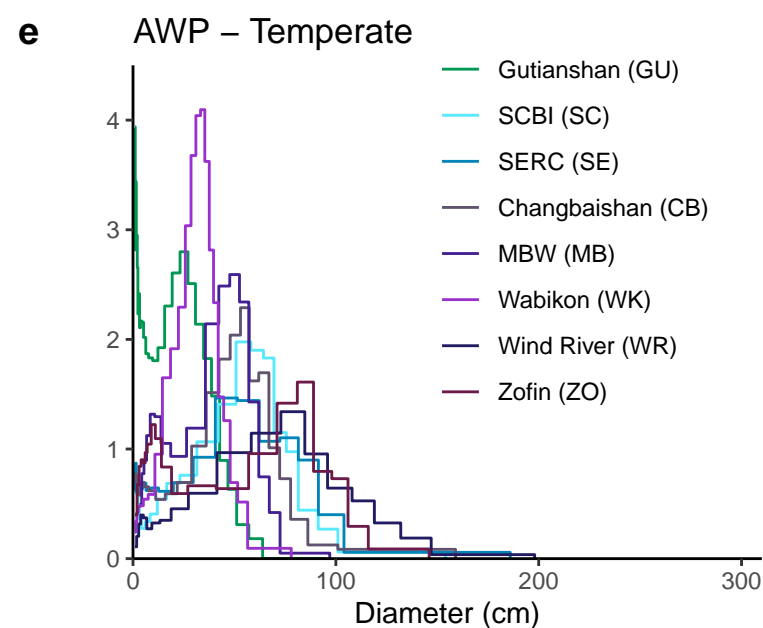
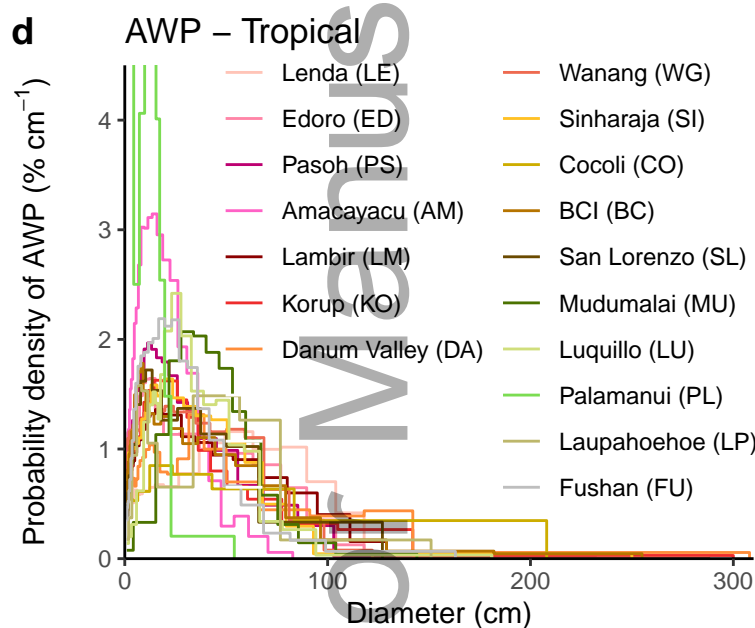
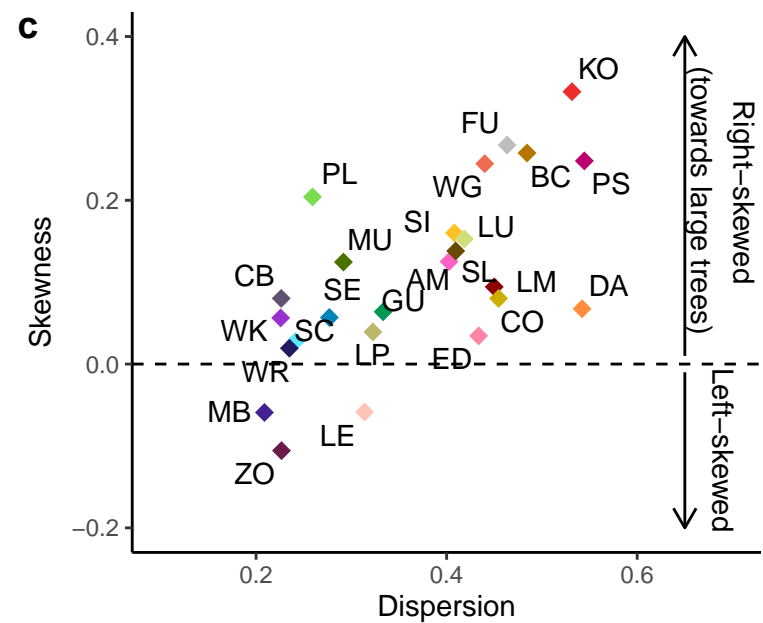
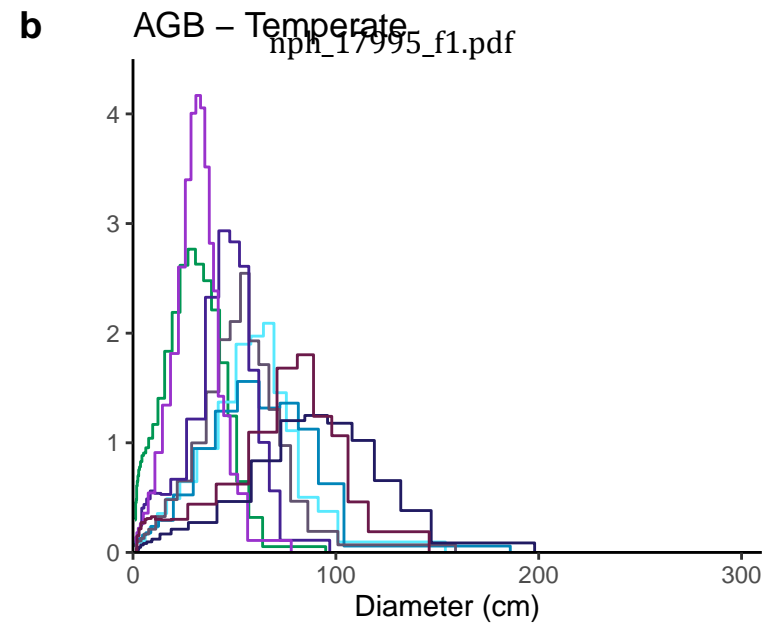
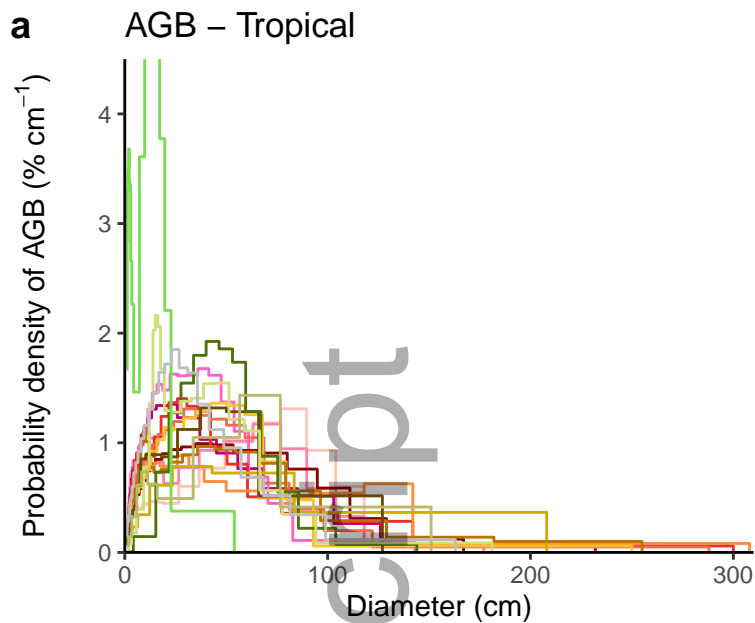
MAP: mean annual precipitation. MAT: mean annual temperature. AGB: aboveground biomass (from the initial census of the focal interval). AWP: aboveground woody productivity. AWM: aboveground woody mortality. MAP and MAT were provided by each site (Anderson-Teixeira *et al.*, 2015; Davies *et al.*, 2021). The census period is the total span of the census years included in this study. AGB, AWP, and AWM are from this study (see Materials and methods section). Values in parentheses correspond to 95% confidence intervals from bootstrapping over 20 x 20 m quadrats with 1000 replicates. Sites are listed in order of absolute latitude. Site name abbreviations: BCI - Barro Colorado Island, MBW - Michigan Big Woods, SCBI - Smithsonian Conservation Biology Institute, SERC - Smithsonian Environmental Research Center. A map of study sites is provided in the Supporting Information Fig. S1.

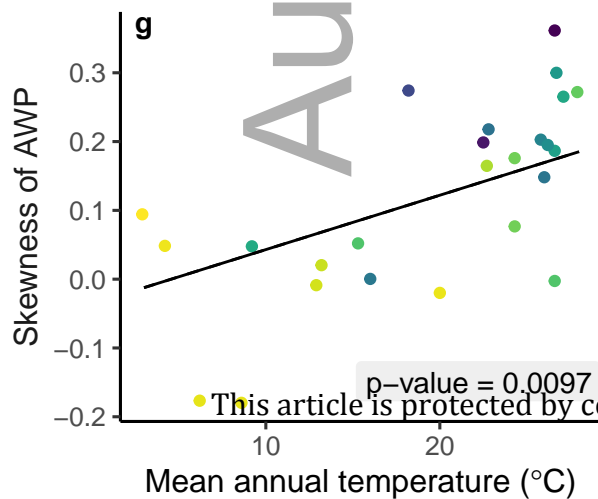
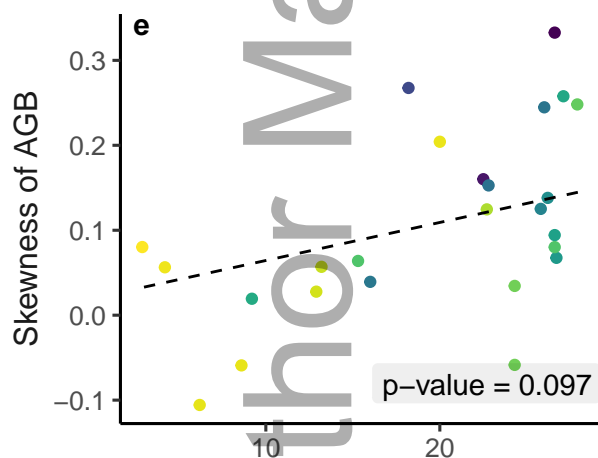
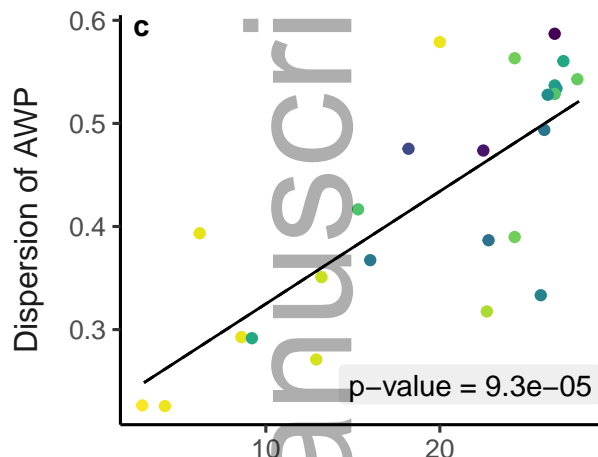
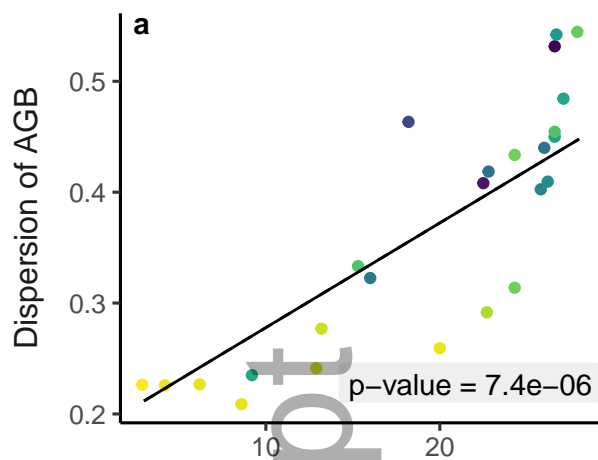
Figure 1: Size-related distributions ($\% \text{ cm}^{-1}$) of above-ground biomass (AGB, in panels a, b), aboveground woody productivity (AWP, panels d,e), and aboveground woody mortality (AWM, panels g, h) in tropical (a,d,g) and temperate (b,e,h) sites, together with among-site variation in the dispersion and skewness of these distributions (c,f,i). Diameter classes for plotting (in a,b,d,e,g,h) vary among sites depending on the number and size distribution of stems (Supporting information, Methods S3); however, analyses are based simply on 1-cm diameter classes (identical across sites). Dispersion is the quartile coefficient of dispersion, defined as the difference between the third and first quartiles, divided by the sum of the first and third quartiles of the distribution; skewness is the nonparametric skew, defined as the mean minus the median, divided by the standard deviation. The legend (d,e) lists sites by absolute latitude (Table 1). The upper limit of the y-axis on graphs of the probability densities (a, b, d, e, g, h) was set to $4.5 \% \text{ cm}^{-1}$ for easier readability, even though it truncates the curve for the Palamanui site (a dry forest with a large proportion of small stems); the untruncated graphs are shown in the Supporting Information (Supporting information, Fig. S11). Graphs for individual sites, with 95% confidence intervals, are presented in the Supporting information, Fig. S10.

Figure 2: Relationships of the dispersion and skewness of aboveground biomass (AGB) and of aboveground woody productivity (AWP) with mean annual temperature (MAT) and mean annual precipitation (MAP). Colors represent the value of the other climate variable: MAP in a,c,e,g and MAT in b,d,f,h. Lines display estimated effects from the multiple linear regressions $\text{dispersion} \sim \text{MAT} + \text{MAP}$ and $\text{skewness} \sim \text{MAT} + \text{MAP}$, and the associated p-values for these effects are shown; the regression lines are represented by solid lines when the p-value is <5% (i.e., the slope is significantly different from zero), and by dashed lines when the p-value is >5%. The full results (including results for the dispersion and skewness of AWM and the medians of all the variables, which have a p-value >5%) are presented in the Supporting information, Table S4.

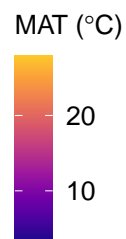
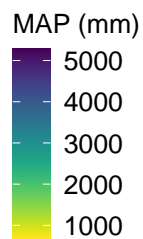
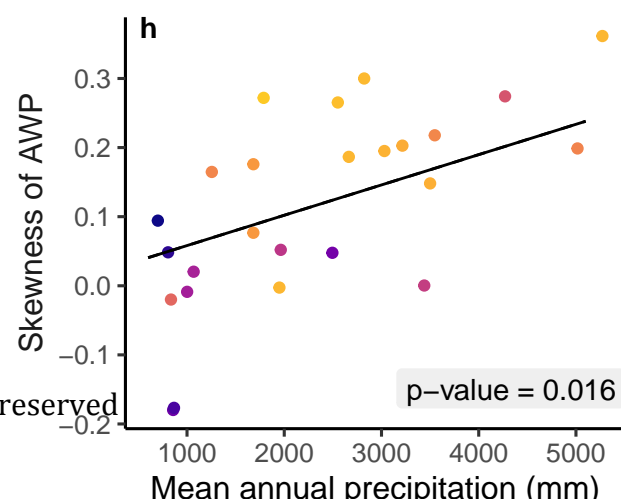
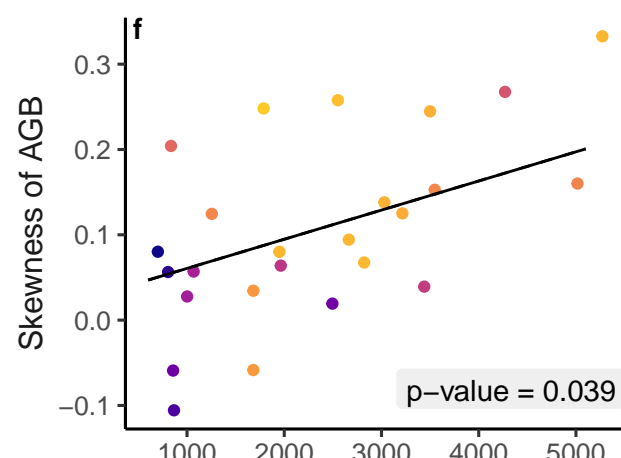
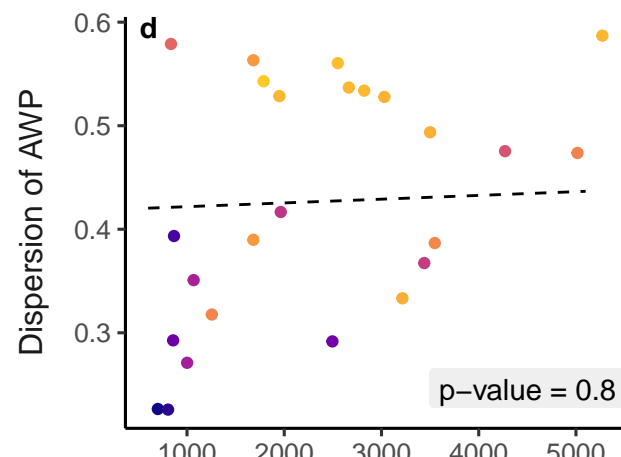
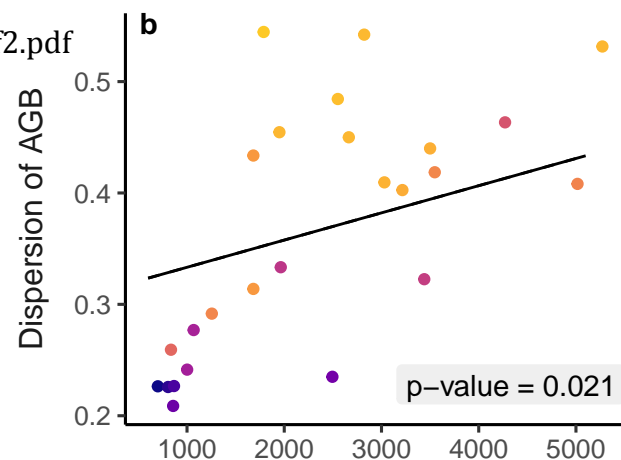
Figure 3: Size-related variation in RAWP (the ratio of aboveground woody productivity to aboveground biomass) and RAWM (the ratio of aboveground woody mortality to aboveground biomass) in tropical (a,c) and temperate (b,d) sites. Sites are listed in order of absolute latitude in the legend, with warm colors for tropical sites, and in cold colors for temperate sites.

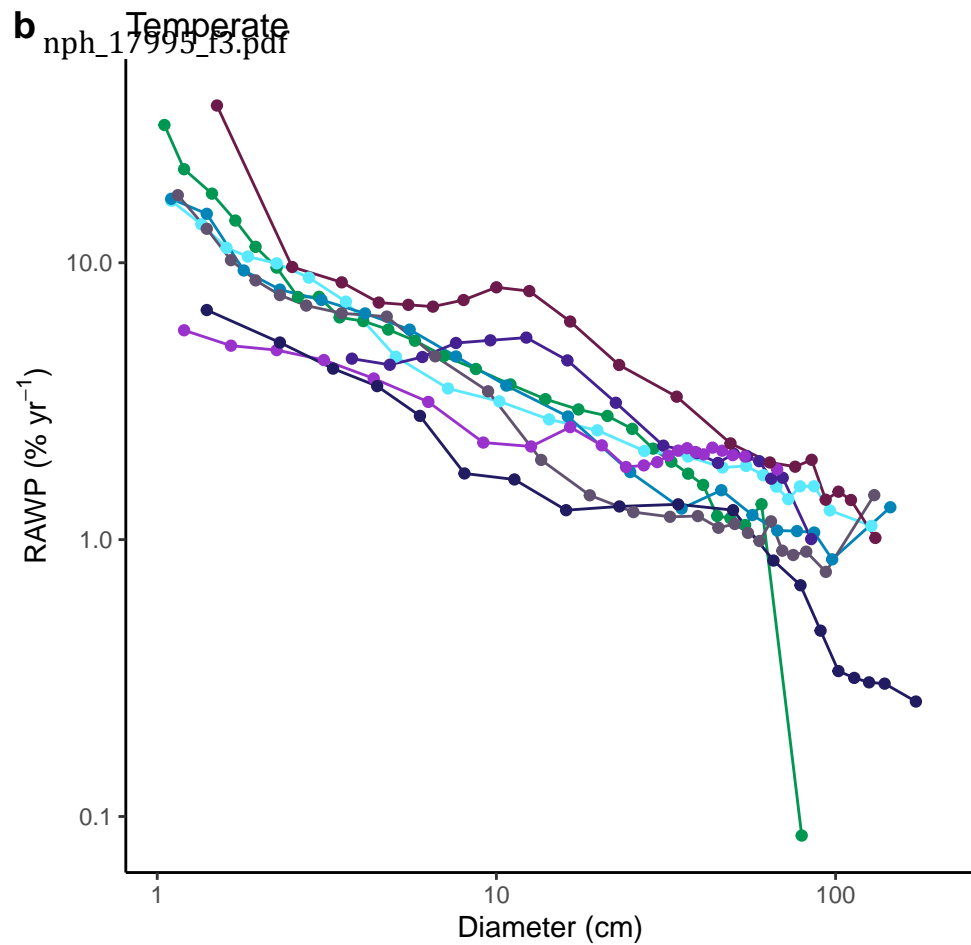
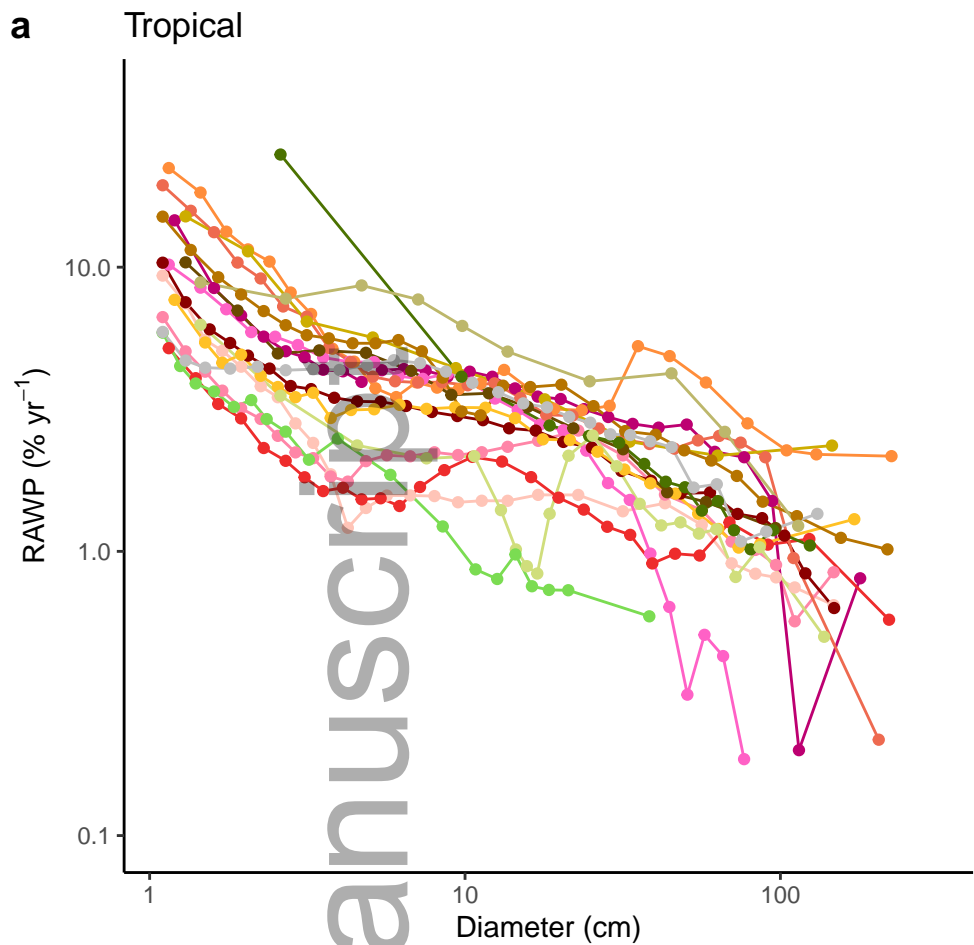
Figure 4: Proportion of biomass stocks and fluxes in (a-b) small ($1 \leq \text{DBH} < 10 \text{ cm}$) and (c-d) large trees ($\geq 60 \text{ cm DBH}$). AGB: aboveground biomass, AWP: aboveground woody productivity, AWM: aboveground woody mortality. Sites are listed in order of absolute latitude in the legend, and are colored in warm colors (red to green) for tropical sites, and in cold colors (green to blue) for temperate sites. Tropical sites are represented by triangles and temperate sites by circles. Error bars represent 95% CIs after bootstrapping 20 x 20 m quadrats with 1000 replicates. Dashed lines correspond to (starting from the top): $y = 2x$, $y = x$, and $y = x/2$. The upper limit of the x- and y-axes on panels (a) and (b) has been set to 0.20 for readability reasons: the full graph (including the Palamanui site) is shown in the Supporting Information (Fig. S12).





nph_17995_f2.pdf





- Lenda
- Eodoro
- Pasoh
- Amacayacu
- Lambir
- Korup
- Danum Valley
- Wanang
- Sinharaja
- Cocoli
- BCI
- San Lorenzo
- Mudumalai
- Luquillo
- Palamanui
- Laupahoehoe
- Fushan
- Gutianshan
- SCBI
- SERC
- Changbaishan
- MBW
- Wabikon
- Wind River
- Zofin

